Organic Electronics 13 (2012) 1377–1381

Contents lists available at SciVerse ScienceDirect

Organic Electronics

journal homepage: www.elsevier.com/locate/orgel

Electric-field controlled light-emissive characteristics in nanoscale for polymer/fullerene organic solar cells

Hyo-min Kim [a], Seok Ho Lee [a], Hak Seob Noh [a], Kihyun Kim [a], Yong-baek Lee [a], Jeongyong Kim [b], Jinsoo Joo [a,*]

[a] Department of Physics, Korea University, Seoul 136-713, Republic of Korea
[b] Department of Physics, University of Incheon, Incheon 406-772, Republic of Korea

ARTICLE INFO

Article history:
Received 17 December 2011
Received in revised form 7 March 2012
Accepted 24 March 2012
Available online 17 April 2012

Keywords:
Electric-field
Photoluminescence
Poly(3-hexylthiophene)
Organic photovoltaic cells
Trap
Nanocharacterization

ABSTRACT

Bulk-hetero-junction (BHJ) organic photovoltaic cells (OPVCs) consisting of a poly(3-hexylthiophene) (P3HT) as a donor and [6,6]-phenyl C_{61} butyric acid methyl ester (PCBM) as an acceptor were fabricated and their light-emissive characteristics as a function of applied bias were investigated. The nanoscale luminescence spectra at different positions on the P3HT/PCBM based photovoltaic cells were measured using a laser confocal microscope (LCM) with a high spatial resolution. For the P3HT/PCBM OPVCs with a relatively thin active layer, the light-emissive characteristics were changed considerably with varying applied bias. We observed that the luminescence intensity increased with increasing reverse bias under light illumination, this result was confirmed by the LCM photoluminescence mapping images. This result originates from the increase of free charges due to the de-trapping effect of trapped charge transfer excitons near the interface, through the external electric-field and incident light.

1. Introduction

Bulk hetero-junction (BHJ) organic photovoltaic cells (OPVCs) using the blending of π-conjugated polymers and fullerene derivatives have been intensively studied with a view to use them in future energy harvesting systems [1,2]. The power conservation efficiency (PCE) of the BHJ-OPVCs has been measured to be as high as 8% [3]. In order to increase of the PCE of the OPVCs, a fundamental understanding of the charge dissociation and transport processes in the composites of the π-conjugated polymers and fullerene derivatives is required. Under light illumination, the photo-generated excitons in π-conjugated polymers are separated through a charge dissociation process at the interface of the donor and acceptor materials, these materials have different electron affinities and ionization energies. In the p-type π-conjugated polymers, the Coulombic binding energy of the excitons is typically in the range of 0.3–0.5 eV [4]. The transport characteristics of the dissociated charges to the electrode through p-type and n-type organic materials are also important for generating electrical power using BHJ-OPVCs. In this way, the PCE of the cells can be determined by looking at the probabilities of exciton diffusion, charge transfer, charge dissociation, and charge collection [5].

The recombination and dissociation processes of charge transfer excitons near the interface of the donor and acceptor materials can be understood in terms of applied bias for increasing the PCE of the BHJ-OPVCs [6–8]. The Onsager-Braun theory [9,10] provides an explanation of the cell characteristics based on the dissociation of the geminate excitons [11–13]. On the other hand, a process involving the non-geminate recombination of electrons and holes was proposed in the Langevin mechanism [14,15] and the Shockley–Read–Hall (SRH) model [16]. Non-geminate recombination can be influenced by trap sites based on

* Corresponding author.
E-mail address: jjoo@korea.ac.kr (J. Joo).

1566-1199/$ - see front matter © 2012 Elsevier B.V. All rights reserved.
http://dx.doi.org/10.1016/j.orgel.2012.03.034

trap-assisted and/or trap-free mechanisms in the material network, as reported by Blom and co-workers [17–19].

Photoluminescence (PL) characteristics can be observed in BHJ-OPVCs when excitons have a low dissociation probability and a high recombination rate. On the other hand, PL quenching and photocurrent have also been generated due to the high dissociation probability of excitons at the donor-acceptor interface and the high transport efficiency of free charges [20]. These processes can be intrinsically and extrinsically controlled by the materials and applied bias, respectively. Increasing the reverse bias for the BHJ-OPVCs reduces the intensity of the charge transfer emissions, which is indicative of the field-induced dissociation probability of charge transfer excitons [21]. In BHJ-OPVCs consisting of p-type poly(3-hexlythiophene) (P3HT) and n-type [6,6]-phenyl-C_{61}-butyric acid methyl ester (PCBM), the emission of the generated excitons and charge transfer excitons (CTE) can be quenched by a high dissociation and transfer probability, estimated to be ~93% and ~100%, respectively [5]. To increase the PCE with a higher dissociation rate, one should also consider the trap states near the donor-acceptor interface. Electric-field-induced luminescence measurement of the BHJ-OPVCs can provide important results for investigating the trap states.

In this study, we report on the electric-field controlled light-emissive characteristics in nanoscale for P3HT/PCBM based BHJ-OPVCs. These characteristics are measured using a laser confocal microscope (LCM) with a high spatial resolution. Fig. 1 shows a schematic illustration of the experimental set-up with the LCM. We observed that in the reverse bias regime, the LCM PL intensity at various positions on the BHJ-OPVCs increased with increasing bias, these results were confirmed by the LCM PL mapping images. The results suggest that the charge transfer excitons were trapped near the interface. In addition, the de-trapped charges through the bias contributed to the increase of the luminescence with an incident light.

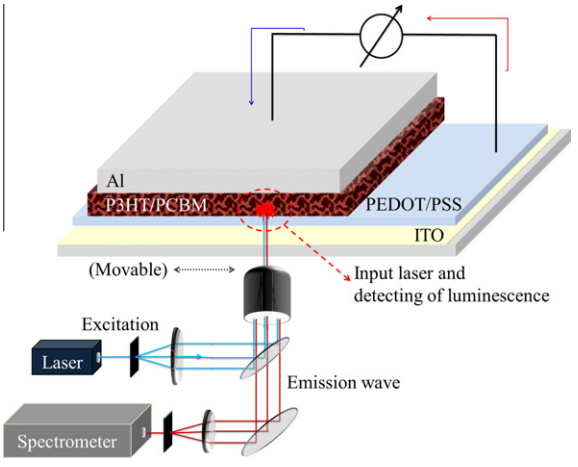

Fig. 1. Schematic illustration of the experimental set-up for electric-field-induced luminescence of P3HT/PCBM OPVCs using a laser confocal microscope (LCM).

2. Experimental

2.1. Fabrication of the P3HT/PCBM based BHJ-OPVCs

The P3HT/PCBM based BHJ-OPVCs were fabricated through typical spin coating and thermal evaporation methods. A poly(3,4-ethylenedioxythiophene)/poly(styrenesulfonate) (PEDOT/PSS) buffer layer was spin-coated onto cleaned and ozone plasma-treated indium tin oxide (ITO) covered glass, and then annealed at 130 °C for 10 min. The active layer of P3HT/PCBM with 1:1 wt% dissolved in chlorobenzene (1 wt%, 1.5 wt% and 3 wt%) was spin-coated onto the PEDOT:PSS layer with different thicknesses of 100 nm (1 wt%), 170 nm (1.5 wt%) and 420 nm (3 wt%). The aluminum (Al) electrode, with a thickness of 75–80 nm, was thermally evaporated at a pressure of less than 10^{-6} torr. Finally, the cells were annealed at 140 °C for 10 min in a glovebox.

2.2. Measurement

The electric-field-induced PL spectra in nanoscale were measured using a LCM (NanoFocusInc. Albatross SPM) to find the time-dependent spectra characteristics. The PL mapping images were obtained using a LCM (WITec Inc. ALPHA300 S). For the LCM PL spectra, the incident laser power was fixed at 50 μW with an excitation wavelength of 488 nm and an acquisition time of 1 s for a single spectra and 40 s for capturing time-dependent spectra characteristics. The focused laser beam from the LCM was about 300 nm, therefore we could perform nanoscale PL measurements. For the LCM PL mapping images, we used a laser with an excitation wavelength of 532 nm. The current density versus voltage (J–V) characteristic curves of the cells were measured using a Keithley 237 SMU combined with a LCM. Fig. 1 shows a schematic illustration of the experimental set-up for the electric-field-induced PL spectra in nanoscale of the BHJ-OPVCs using the LCM system.

3. Results and discussion

Fig. 2[1] shows the J–V characteristic curves of the P3HT/PCBM BHJ-OPVCs. The J_{dark}(black curve) and J_{light}(red curve) were measured under dark and light conditions, respectively. The photocurrent J_{ph}(green curve) is defined by $|J_{light} - J_{dark}|$. We observed the photovoltaic characteristics of the cells, the monochromatic PCE was estimated to be about 5.1% under illumination by monochromatic LED with a wavelength of 505 nm. The short circuit current density (J_{sc}) was 2.6 mA/cm^2 and the open circuit voltage (V_{oc}) was 0.4 V. In the reverse bias region, J_{dark} slowly increased with increasing the bias from −1 V to −3 V, based on the SRH model [22,23], this indicates the widening of the depletion region and charge generation (or charge trap) through generated trap states due to oxidation, defects, disorder, and/or surface imperfections at the donor-acceptor interface. The J_{ph} was increased due to

[1] Please note that Fig. 2 will appear in B/W in print and color in the web version. Based on this, please approve the footnote 1 which explains this.

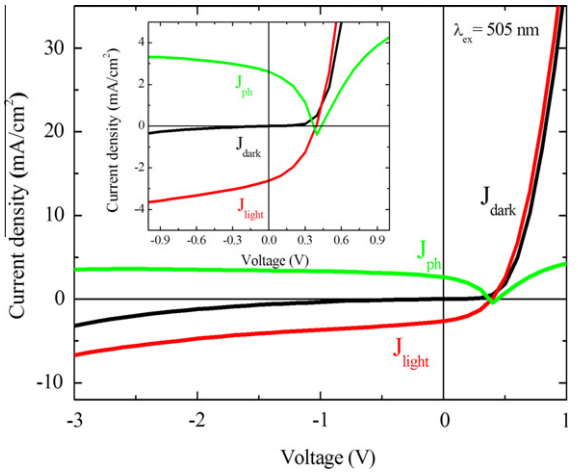

Fig. 2. *J–V* characteristic curves (J_{dark}, J_{light} and J_{ph}) for P3HT/PCBM OPVCs between −3 V and +1 V under monochromatic LED conditions (λ_{ex} = 505 nm). Inset: magnification of the *J–V* characteristic curves from −1 to +1 V.

the increase of the dissociation probability of charge transfer excitons by the electric-field. And, as shown in Fig. 2, the J_{ph} was saturated to a value of 3.49 mA/cm^2 above −1.5 V when all bound electron-hole pairs were dissociated in the donor-acceptor interface [21].

Fig. 3 (a) shows LCM PL spectra with varying applied voltages for the P3HT/PCBM OPVCs with a 100 nm active layer. We observed a considerable increase of the LCM PL intensity as the reverse bias was increased. The LCM PL emission peaks from the P3HT/PCBM OPVCs were detected at 651 nm and 720 nm. The observed peaks at 651 nm and 720 nm correspond to the optical characteristics of the P3HT and P3HT/PCBM blend, respectively [24]. The positions of the LCM PL peaks were not changed by the applied bias, indicating no contribution to the observed PL from the charge transfer exciton emission. The LCM PL intensity at 651 nm gradually increased from 3%, 20%, 43–59% with an increasing bias of −1 V, −2 V, −3 V and −4 V, respectively. This behavior was repeatedly observed in the same cells, indicating the heating effects are negligible. The similar results were also observed for the cells with a 170 nm active layer. On the other hand, the electroluminescence (EL) in the reverse bias regime was not observed for these cells (not shown in here) because there were large injection barriers for hole and electrons in reverse bias. The inset of Fig. 3 (a) shows correlation between PL intensity and electric-field with various thicknesses of active layer. The normalized field-dependent PL intensity $Q(F)$ were obtained from the experimental PL intensity $I(F)$ and the zero field PL intensity $I(0)$ using the equation $Q(F) = [I(F) - I(0)]/I(0)$. The LCM PL intensities were considerably changed with applying high electric-field (above $\sim 10^7$ V/m) for the OPVCs with relatively thin active layers (e.g., 100 nm and 170 nm), while they were not much changed with applying low electric-field (below $\sim 7 \times 10^6$ V/m) for all OPVCs studied here.

In general, for ideal BHJ-OPVCs, the quenching of the charge transfer emission has been observed after the

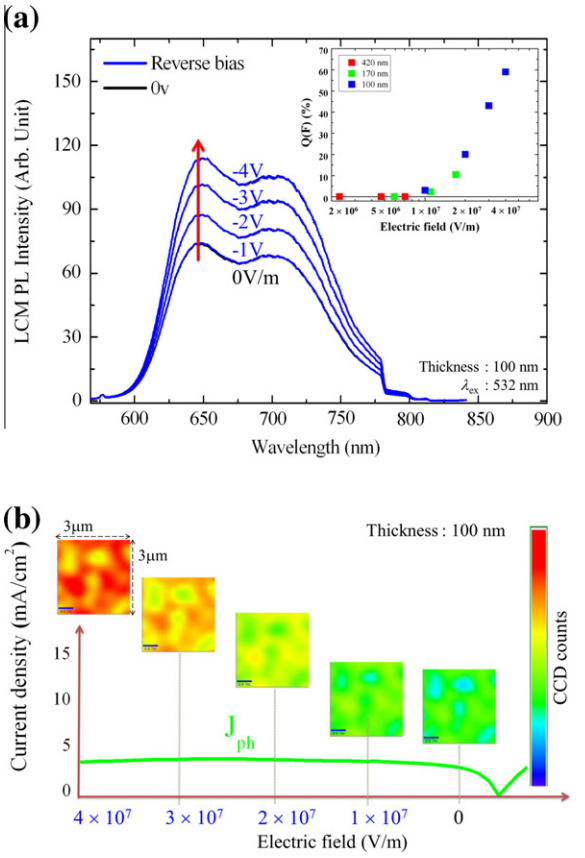

Fig. 3. (a) LCM PL spectra of P3HT/PCBM OPVCs with various reverse biases. Inset: normalized LCM PL intensity versus applied electric-field of the OPVCs with various thicknesses of active layer. (b) LCM PL mapping images and photocurrent density of P3HT/PCBM OPVCs with various reverse electric-fields (Scan size: 3 μm × 3 μm). The color scale bar on the right represents the relative PL intensity in terms of photon count. (For interpretation of the references to colour in this figure legend, the reader is referred to the web version of this article.)

increase of the dissociation probability of charge transfer excitons at the donor-acceptor interface. The charge transfer emission increases with decreasing exciton dissociation probability, this, in turn, can be controlled by an electric-field in the reverse bias region [25,26]. However, our results suggest different causes for the PL enhancement with increasing reverse bias, for example, the de-trapping effect and additional charge generation by the electric-field. This will be further discuss with the analysis from Fig. 6.

Fig. 3(b) shows the LCM PL mapping images (right *y*-axis) and photocurrent density (left *y*-axis) of the P3HT/PCBM OPVCs at different applied electric-fields. The color scale bar on the right in Fig. 3(b) represents the integrated PL intensity in terms of photon counts for the wavelength region of 500–900 nm. We visually confirmed the increase of the nanoscale PL intensity with increasing reverse bias from the cells, as shown in Fig. 3 (b). However, the photocurrent (J_{ph}) was saturated with the applied electric-field above $\sim 1 \times 10^7$ V/m. These results suggest that the enhanced luminescence did not originate from photocurrent

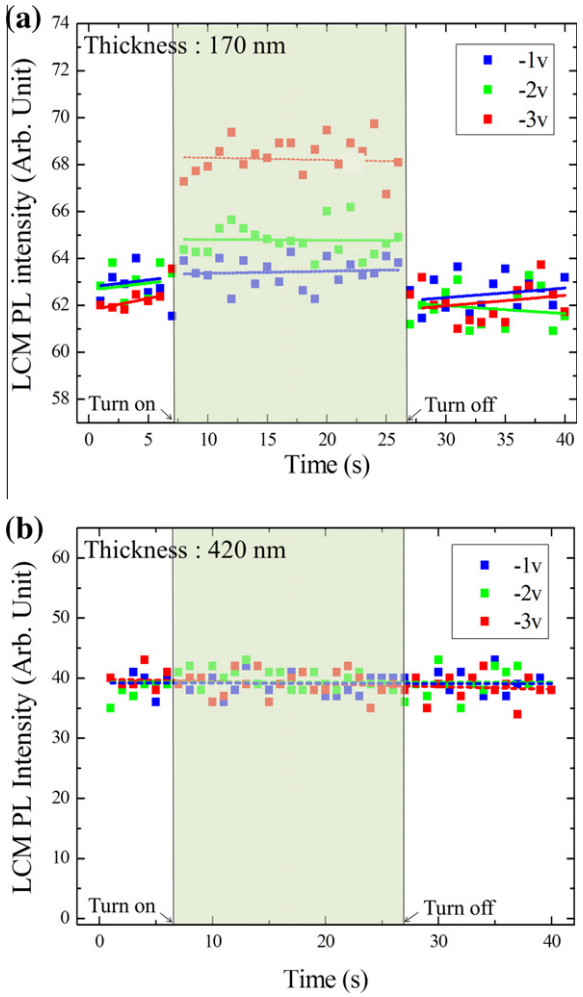

Fig. 4. LCM PL intensities at 651 nm as a function of light irradiation time with various reverse bias for the cells: (a) thickness of active layer was 170 nm and (b) thickness of active layer was 420 nm.

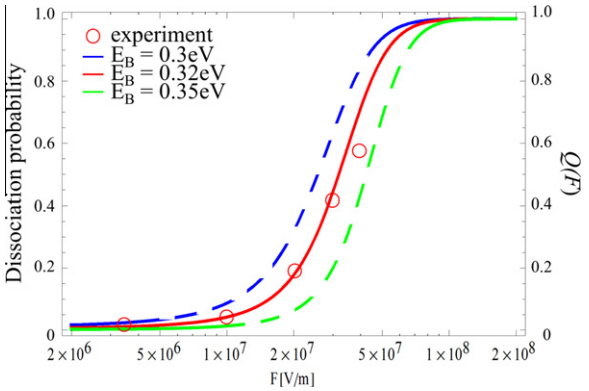

Fig. 5. Dissociation probability versus applied electric-field of P3HT/PCBM OPVCs based on the Onsager-Braun theory. The solid curves show the theoretical results and the open circles show the experimental results.

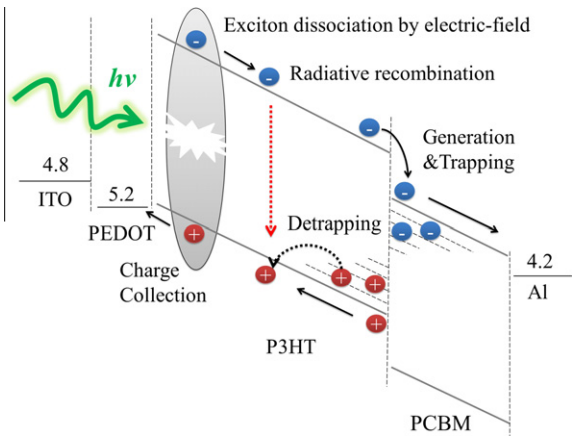

Fig. 6. Schematic illustration of the de-trapping effect by an applied electric-field in reverse bias condition.

loss. The inhomogeneous colors of the PL mapping images of the cells should also be noted; this indicates spatially inhomogeneous light-emissions from the P3HT/PCBM blend. Similar PL mapping images were also detected at different spots on the same solar cell.

Fig. 4 shows the variation of LCM PL intensity as a function of light irradiation time for P3HT/PCBM OPVCs with different thicknesses of active layers. The thicknesses of the active layers of two different BHJ-OPVCs used were measured to be about 170 nm (1.5 wt%) and 420 nm (3 wt%). The applied bias of the cells was turned on and off at 7 s and 27 s, respectively, and the LCM PL intensity at 651 nm was measured at different reverse biases. It should be noted that the PL spectra have the same shape as those in Fig. 3 (a). As shown in Fig. 4, the LCM PL intensity was considerably and immediately changed up to 10.4% at −3 V with light irradiation of the cells with the thin active layer (thickness = 170 nm), while it was not changed for the cells with the thick active layer (thickness = 420 nm). As the reverse bias increased, the LCM PL intensity of the cells with the thin layer increased, as shown in Fig. 4 (a). For the OPVCs with the thicker active layer, the absolute value of applied electric-field was relatively weaker compared to that of the thin cells. Therefore, we could not observe variations in the PL intensity. These results indicate the existence of an optimal thickness for the active layer of BHJ-OPVCs when observing field-induced PL.

The dissociation probability of the photo-generated excitons depends on the applied bias, i.e., the electric-field. We calculated the field dependent dissociation yield of the excitons based on the Onsarger-Braun theory [27]. In this theory, the field (F) dependent dissociation rate $k_d(F)$ is described by:

$$k_d(F) = \frac{3\gamma}{4\pi r_s^3} \exp\left(-\frac{E_b}{k_B T}\right) \frac{J_1(2\sqrt{-2b})}{\sqrt{-2b}}$$

where F is the electric-field, r_s is the initial exciton radius, $E_b = e^2/(4\pi\varepsilon\varepsilon_0 r_s)$ is the exciton binding energy, $k_B T$ is the thermal energy, J_1 is the first order of Bessel function, $b = e^3 F/[8\pi\varepsilon\varepsilon_0 (k_B T)^2]$, $\gamma = e\mu/\varepsilon\varepsilon_0$ is the Langevin recombina-

tion factor ($\varepsilon\varepsilon_0$ is the effective dielectric constant of the polymer) [28]. The exciton dissociation probability (D.P.) can be determined by [29]:

$$\text{D.P.} = \frac{k_d(F)}{k_d(F)+k_f} = \frac{\kappa_d(F)}{\kappa_d(F)+(\mu\tau_f)^{-1}} \quad \text{with}$$

$$k_d(F) \equiv \mu\kappa_d(F),$$

Here μ is the sum of the electron and hole mobility, $\tau_f(=k_f^{-1})$ is the exciton lifetime. Using this equation with $\mu\tau = 5\times10^{-16}\ m^2/V$ and $\varepsilon = 3.4$ [30], the theoretical solid curves for the D.P. were obtained as a function of electric-field, as shown in Fig. 5. The normalized field-dependent PL intensity $Q(F)$ was calculated from the experimental LCM PL intensity of the OPVCs with various thicknesses (100 nm, 170 nm, and 420 nm) as shown in the inset of Fig. 3 (a). The experimental data (open circles in Fig. 5) $Q(F)$ were well fitted to the theoretical curve when the binding energy was 0.32 eV, which is the exciton binding energy in P3HT materials.

The increase of the LCM PL intensity with increasing the reverse bias indicates the enhancement of the radiative recombination process and the creation of more excitons. From the results in Fig. 3 (b), we also observed that the photocurrent was saturated with increasing electric-field, while the LCM PL intensity increased. To analyze these results, we should first consider the correlation of the applied electric-field with dissociated excitons and the regenerated free charges for singlet excitons. We propose a model of the de-trap induced PL enhancement, as shown in Fig. 6. For exciton dissociation and charge transport in BHJ-OPVCs, we must consider the trap sites in the active layer. The trap states often mainly exist at nanojunctions of the P3HT and PCBM interface due to oxidation, defects, disorder, and/or imperfections [17–19]. Under illumination, charge transfer excitons can be formed at the donor and acceptor interface, some of these (mainly non-trapped holes and electrons) are then dissociated and transported to electrodes. However, some of the charge transfer excitons can be trapped in the trap sites, as shown in Fig. 6. The trapped charges are escaped from the trap sites through the applied high electric-field, i.e., the de-trapping effect. At the same time, photo-generated excitons are dissociated by electric-field before reaching at P3HT/PCBM interface, resulting in the generation of additional free electrons and holes. The radiative recombination probability increases due to additional charges that were de-trapped holes and dissociated electrons, by electric-field. These can contribute to induce more excitons to increase the PL intensity as the bias increases.

4. Conclusion

P3HT/PCBM bulk-hetero-junction organic photovoltaic cells were fabricated and used to study electric-field-induced PL variation. The nanoscale LCM PL intensity for the cells increased with increasing reverse bias, this was confirmed by LCM PL mapping images. The photocurrent of the OPVCs was saturated with applying high electric-field. Using these results, the exciton binding energy in the P3HT materials was estimated to be 0.32 eV. We propose the existence of trap states at the interface, and further, that the de-trapping of charge transfer excitons by the applied electric-field contributed to the increase of PL intensity of the photovoltaic cells.

Acknowledgment

This work was supported by a National Research Foundation (NRF) of Korea grant funded by the Korean government (MEST) (No. R0A-2007-000-20053-0).

References

[1] J.J.M. Halls, C.A. Walsh, N.C. Greenham, E.A. Marseglla, R.H. Friend, S.C. Moratti, A.B. Holmes, Nature 376 (1995) 498–500.
[2] G. Yu, J. Gao, J.C. Hummelen, F. Wudl, A.J. Heeger, Science 270 (1995) 1789–1791.
[3] M.A. Green, K. Emery, Y. Hishikawa, W. Warta, Prog. Photovolt.: Res. Appl. 19 (2011) 84–92.
[4] J.J.M. Halls, J. Cornil, D.A. dos Santos, R. Silbey, D.-H. Hwang, A.B. Holmes, J.L. Brédas, R.H. Friend, Phys. Rev. B 60 (1999) 5721–5727.
[5] J. Guo, H. Ohkita, H. Benten, S. Ito, J. Am. Chem. Soc. 132 (2010) 6154–6164.
[6] V.D. Mihailetchi, L.J.A. Koster, J.C. Hummelen, P.W.M. Blom, Phys. Rev. Lett. 93 (2004) 216601.
[7] D. Veldman, Ö. İpek, S.C.J. Meskers, J. Sweelssen, M.M. Koetse, S.C. Veenstra, J.M. Kroon, S.S. van Bavel, J. Loos, R.A.J. Janssen, J. Am. Chem. Soc. 130 (2008) 7721–7735.
[8] A. Liu, S. Zhao, S.-B. Rim, J. Wu, M. Könemann, P. Erk, P. Peumans, Adv. Mater. 20 (2008) 1065–1070.
[9] C.L. Braun, J. Chem. Phys. 80 (1984) 4157–4161.
[10] M. Wojcik, M. Tachiya, J. Chem. Phys. 130 (2009) 104107.
[11] K. Maturová, S.S. van Bavel, M.M. Wienk, R.A.J. Janssen, M. Kemerink, Nano Lett. 9 (2009) 3032–3037.
[12] R.A. Marsh, C.R. McNeill, A. Abrusci, A.R. Campbell, R.H. Friend, Nano Lett. 8 (2008) 1393–1398.
[13] J. Szmytkowski, Semicond. Sci. Technol. 25 (2010) 015009.
[14] L.J.A. Koster, V.D. Mihailetchi, P.W.M. Blom, Appl. Phys. Lett. 88 (2006) 052104.
[15] G. Juška, K. Genevičius, G. Sliaužys, N. Nekrašas, R. Österbacka, J. Non Cryst. Solids. 354 (2008) 2858.
[16] R.A. Street, M. Schoendorf, A. Roy, J.H. Lee, Phys. Rev. B 81 (2010) 205307.
[17] M.M. Mandoc, F.B. Kooistra, J.C. Hummelen, B. de Boer, P.W.M. Blom, Appl. Phys. Lett. 91 (2007) 263505.
[18] G.A.H. Wetzelaer, M. Kuik, M. Lenes, P.W.M. Blom, Appl. Phys. Lett. 99 (2011) 153506.
[19] G.A.H. Wetzelaer, L.J.A. Koster, P.W.M. Blom, Phys. Rev. Lett. 107 (2011) 066605.
[20] K. Kim, J.W. Lee, Y.B. Lee, E.H. Cho, H.-S. Noh, S.G. Jo, J. Joo, Org. Electron. 12 (2011) 1695–1700.
[21] Y. Zhou, K. Tvingstedt, F. Zhang, C. Du, W.-X. Ni, M.R. Andersson, O. Inganäs, Adv. Funct. Mater. 19 (2009) 3293–3299.
[22] C. Deibel, V. Dyakonov, Rep. Prog. Phys. 73 (2010) 096401.
[23] R.A. Street, S. Cowan, A.J. Heeger, Phys. Rev. B 82 (2010) 121301.
[24] S.S. van Bavel, M. Bärenklau, G. de With, H. Hoppe, J. Loos, Adv. Funct. Mater. 20 (2010) 1458–1463.
[25] S. Inal, M. Schubert, A. Sellinger, D. Neher, J. Phys. Chem. Lett. 1 (2010) 982–986.
[26] J.M. Lupton, C. Im, H. Bässler, J. Phys. D: Appl. Phys. 36 (2003) 1171–1175.
[27] L. Onsager, Phys. Rev. 54 (1938) 554–557.
[28] A. Pivrikas, G. Juška, R. Österbacka, M. Westerling, M. Vilinas, K. Arlauskas, H. Stubb, Phys. Rev. B 71 (2005) 125205.
[29] C. Deibel, T. Strobel, V. Dyakonov, Phys. Rev. Lett. 103 (2009) 036402.
[30] P.E. Shaw, A. Ruseckas, I.D.W. Samuel, Adv. Mater. 20 (2008) 3516–3520.